Thermochimica Acta 503–504 (2010) 136–140

Contents lists available at ScienceDirect

Thermochimica Acta

journal homepage: www.elsevier.com/locate/tca

Short communication

# Synthesis and growth thermodynamic studies of CdS nanocrystals using isothermal titration calorimetry

Junying Jiang[a], Zaiyin Huang[a,*], Qi Xiao[b], Yi Liu[b], Yan Mi[a], Yanfen Li[a]

[a] College of Chemistry and Ecological Engineering, Guangxi University for Nationalities, 188 Daxue East Road, Nanning 530006, PR China
[b] College of Chemistry and Molecular Sciences, Wuhan University, Wuhan 430072, PR China

ARTICLE INFO

*Article history:*
Received 16 December 2009
Received in revised form 4 March 2010
Accepted 10 March 2010
Available online 18 March 2010

*Keywords:*
CdS nanocrystal
Controlled synthesis
Thermodynamic data

ABSTRACT

A simple and facile solution-phase method has been developed for the fabrication and growth thermodynamic studies of CdS nanocrystals (NCs) using isothermal titration calorimetry (ITC). Monodispersed and uniform CdS NCs with diameter less than 10 nm have been successfully obtained by controlling the preparation conditions. Meanwhile, the growth thermodynamic properties were observed in situ using ITC. Studying on the thermodynamics of nanomaterials makes significant advances in our understanding of its growth mechanism, as well as the correlation between thermodynamic data and structure. Optimization process of synthesizing target nanomaterials can also be realized.



## 1. Introduction

Many physical properties of nanostructured semiconductors depend strongly on their size, shape, and crystal structure [1]. Therefore, the development of well-controlled synthetic methods for tailoring micro/nanocrystals shape and elucidation of the mechanisms are important issues in nanomaterials chemistry [2–4]. As an important II–VI group semiconductor with a narrow band gap, CdS is useful for many important applications, such as light emitting diodes, flat panel displays, solar cells, optical devices, laser, photocatalysts, and diagnostic tool [5–14]. So far, big efforts have been devoted to the synthesis of CdS nanostructures with different morphologies, including solvothermal and hydrothermal method [15–17], solution method [18], vapor–liquid–solid-assisted method [19], colloidal micellar method [20], electrochemical process [21], and several different self-assembly processes [22,23]. However, these methods need severe conditions or complicated equipment, or have difficulty in controllability and repeatability. The development of a facile preparation route could favor and speed up the application of CdS nanomaterials.

Elucidation of the energetic principles of binding affinity and specificity is a central task in many branches of current sciences, such as biology, medicine, pharmacology, chemistry, and material sciences. ITC is a valuable experimental tool for the facilitating quantification of the thermodynamic parameters that characterize recognition processes involving biomacromolecule and chemical reactions. The method provides access to all relevant thermodynamic information by performing a few experiments. In particular, ITC experiments allow to bypass tedious and rarely precise procedures aimed at determining the changes in enthalpy and entropy upon binding by Van't Hoff analysis. ITC, being the "gold standard", has been widely used in biologically oriented fields [24]. In biologically relevant context, ITC, for instance, is mainly used to complement structural data by measuring the affinity of diverse ligands to proteins [25,26]. Analysis of mutant complexes or measurements with closely related compounds allows the identification of energetically important contacts [27]. Nevertheless, the use of ITC is by no means limited to biomedical applications. Admittedly, ITC can also enrich the arsenal of experimental tool in almost all branches of the chemical sciences, and many branches of the material science. It also has been used to investigate the heat change associated with the growth or assembly of nanomaterials [28–30]. The science underpinned by ITC data is of exceptional value in understanding the correlation between thermodynamic data and molecular structural details related to a change from one state to another. We can see thermodynamic data are being fed into the lead optimization process to help steer decisions on compound design. Therefore, ITC is a very simple and feasible method to find the best conditions of fabricating target products, as well as thoroughly understand the nature and mechanism of synthesizing nanomaterials.

In view of the limited knowledge of the growth mechanism of semiconductor NCs and the key role of thermodynamics, we considered it is important to investigate the growth thermodynamics of CdS NCs by ITC. Herein, we have successfully fabricated well-

* Corresponding author. Tel.: +86 771 3262120; fax: +86 771 3261718.
*E-mail address:* hzy210210@163.com (Z. Huang).

0040-6031/$ – see front matter © 2010 Elsevier B.V. All rights reserved.
doi:10.1016/j.tca.2010.03.010

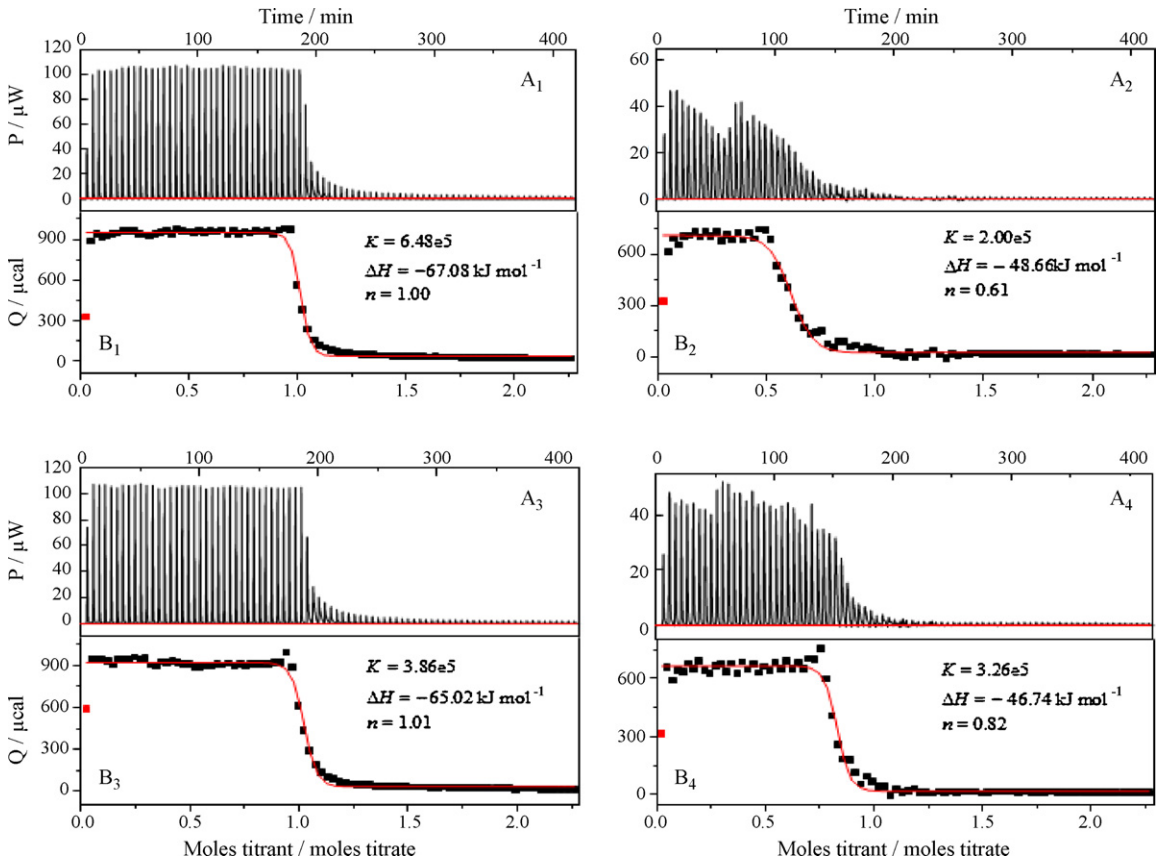


**Fig. 1.** $A_1$ and $A_2$: Isothermal titration calorimetry profiles for $Cd^{2+}$ binding of $S^{2-}$ in ultrapure water and in ethylene glycol at 25 °C, respectively. $B_1$ and $B_2$: Heat evolved (μcal) against the molar ratio of $S^{2-}$ to $Cd^{2+}$ corresponding to the ITC. $A_3$ and $A_4$: Isothermal titration calorimetry profiles for $Cd^{2+}$ binding of $S^{2-}$ in ultrapure water and in ethylene glycol at 31 °C, respectively. $B_3$ and $B_4$: Heat evolved (μcal) against the molar ratio of $S^{2-}$ to $Cd^{2+}$ corresponding to the ITC.

defined and uniform CdS NCs with mean diameter less than 10 nm and investigated its growth thermodynamics through this method. The variation of thermodynamic functions under different parameters, such as temperature and solvents was discussed. The possible reasons of the change were also discussed.

## 2. Experimental

Cadmium nitrate ($Cd(NO_3)_2{\cdot}4H_2O$, ≥99.0% purity) and sodium sulfite ($Na_2S{\cdot}9H_2O$, ≥98.0% purity) were purchased from Tianjin Kermel Chemical Reagents Development Centre. Ethylene glycol (CAS No. 107-21-1) and ethanol absolute (≥99.7% purity) were from Xilong Chemical Industrial Company. All these chemical reagents were used without further purification or drying. Water used was of ultrapure quality.

The growth of CdS NCs and ITC experiments were performed using a TA Instrument nano ITC 2G instrument at 25 °C and 31 °C. The instrument consists of two identical cells, one for sample and the other for reference [31]. Before the measurements, all the solutions were degassed under vacuum while stirring. In a typical titration, with stirring at 300 rpm, 3 μL 20 mmol aqueous solution of $Na_2S$ taken in the syringe was injected in equal intervals of 5 min to the $Cd(NO_3)_2$ aqueous solution (2.5 mmol) which was taken in the sample cell with 1.0 mL capacity. A total of 250 μL $Na_2S$ solution was added to $Cd(NO_3)_2$ solution. The reference cell of the microcalorimeter was filled with ultrapure water and both of the cells were maintained at the same temperature. When $Na_2S$ solution was injected to $Cd(NO_3)_2$, the difference in heat needed to keep both the sample cell and reference cell at the same temperature was monitored. To calibrate the heat effects of dilution and mixing, the control experiments were performed by injecting the $Na_2S$ solution into ultrapure water under the same conditions and subtracted from the experimental data. The heat released by the dilution of $Cd(NO_3)_2$ was negligible. For the contrast experiments, ultrapure water was substituted by ethylene glycol, keeping the other conditions constant.

Calorimetric data for $Cd^{2+}$ binding of $S^{2-}$ were analyzed using the NanoAnalyze software for ITC as provided by TA Instrument. The intrinsic molar enthalpy change ($\Delta H$), the binding stoichiometry ($n$) and binding constant ($K$) for the binding process were obtained from the best fit of the calorimetric data. The Gibbs free energy change ($\Delta G$) and the entropy change ($\Delta S$) of binding were calculated from $K$ and $\Delta H$ using the fundamental equations of thermodynamics: (1) $\Delta G = -RT\ln K$; (2) $\Delta S = (\Delta H - \Delta G)/T$; (3) $\Delta A = \Delta G$ (both the concentrations of $Cd(NO_3)_2$ and $Na_2S$ solutions are so small that the slight difference in volume resulting from mixing was negligible. Thus, we can consider the system presents a constant volume). After the titration, the precipitate was harvested by centrifugation and washed several times with ultrapure water and absolute ethanol and then dried in vacuum at room temperature. The as-prepared products were further characterized by X-ray diffraction (XRD) using an X-ray diffractmeter (the Philips X'Pert) with Cu Kα radiation (λ = 1.5406 Å), transmission electron microscopy (TEM; JEOL JEM-2010), thermogravimetric analysis (TGA) and differential thermal analysis (DTA) using simultaneous thermal analyzer (NETZSCH STA 409 PC/PG) with a heating rate of 10 °C $min^{-1}$ in flowing nitrogen gas (30 mL $min^{-1}$). Sample mass in the TG/DTA analysis was 23.862 mg and the temperature range is from room temperature (23 °C) to 850 °C.

**Table 1**
Thermodynamic parameters for the binding of $S^{2-}$ to $Cd^{2+}$ measures by ITC.

| Temperature (°C) | Solvent | $K$ ($10^5$ L mol$^{-1}$) | $\Delta G = \Delta A$ (kJ mol$^{-1}$) | $\Delta H$ (kJ mol$^{-1}$) | $\Delta S$ (J K$^{-1}$ mol$^{-1}$) | $n$ |
|---|---|---|---|---|---|---|
| 25 | Ultrapure water | 6.48 ± 0.01 | −33.207 ± 0.002 | −66.89 ± 0.19 | −112.77 ± 0.70 | 1.04 ± 0.04 |
| | Ethylene glycol | 2.05 ± 0.05 | −30.347 ± 0.054 | −48.29 ± 0.39 | −60.10 ± 1.43 | 0.62 ± 0.01 |
| 31 | Ultrapure water | 3.84 ± 0.02 | −32.603 ± 0.064 | −64.60 ± 0.42 | −105.08 ± 1.17 | 1.03 ± 0.02 |
| | Ethylene glycol | 3.15 ± 0.11 | −32.045 ± 0.092 | −47.05 ± 0.31 | −49.28 ± 1.32 | 0.77 ± 0.06 |

## 3. Results and discussion

### 3.1. ITC analyses

ITC profile for $Cd^{2+}$ binding of $S^{2-}$ is shown in Fig. 1. $A_1$, $A_2$, $A_3$, $A_4$ are representatively raw ITC curves resulting from the injections of $Na_2S$ solution into $Cd(NO_3)_2$ solution. The areas above these heat burst curves were determined by integration to yield the associated injection heats. These injection heats were corrected by subtracting the corresponding dilution heats. With the injection of $S^{2-}$, the exothermic changed gradually and approached to those of simple dilution of $S^{2-}$ into the buffer, indicating that the binding reaction was almost completed. $B_1$, $B_2$, $B_3$, $B_4$ show the resulting corrected injection heats plotted as a function of the ratio of $[S^{2-}]/[Cd^{2+}]$, in which the data points reflect the experimental injection heats, while the solid line reflects the calculated fit of the data with a model for a single set of identical sites [32]. The model employed in the fit was the one that yielded a reasonable fit of the experimental data. Experiments were repeated twice and the data set from each experiment were regressed independently. The thermodynamic parameters $\Delta H$, $\Delta G$, $\Delta A$, $\Delta S$, $n$ and $K$ obtained from our ITC experiments are summarized in Table 1.

Inspection of these thermodynamic data in Table 1, we can see, (1) negative $\Delta G$, $\Delta H$ and positive $K$ values suggest that the binding process is exothermic. $\Delta S$ is negative mainly because of the binding of $Cd^{2+}$ and $S^{2-}$ which results that the free ions in the system become less. (2) When the temperature is stationary, the $\Delta G$, $\Delta H$, $\Delta S$ values in water are smaller while $K$ and $n$ are larger than in ethylene glycol indicating the binding affinities of $S^{2-}$ and $Cd^{2+}$ in water are more powerful. (3) When the solvent is water, the value of $K$ decreases and $\Delta G$, $\Delta H$, $\Delta S$ values increase with the temperature building-up which corresponds to the rule that the higher temperatures go against the exothermic reactions. However, when ethylene glycol is the solvent, the results show a contrast and the $n$ value is larger suggesting that a higher temperature boosts the binding reaction. The possible reason is that the dissociations of $Na_2S$ and $Cd(NO_3)_2$ in ethylene glycol are more difficult and inexhaustive. When the temperature is elevated, more $S^{2-}$ and $Cd^{2+}$ are released and increase the binding probability. However, when in water, almost all the reactants can be dissociated and the effect of temperature is negligible. (4) The $n$ values for different solvents indicate that each $S^{2-}$ binds to one $Cd^{2+}$ in water while in ethylene glycol the binding ratio is lower.

From ITC studies, we obtained the overall thermodynamic parameters and found the difference between different conditions. Information obtained from this study will be helpful to find the best conditions for our experiments.

### 3.2. TG/DTA analyses

The simultaneous TG–DTA curve of CdS NCs synthesized in ultrapure water at 31 °C is shown in Fig. 2. The first mass loss observed below 120 °C, corresponding to the endothermic peak at about 100 °C, is due to the loss of adsorbed water and ethanol, with loss of 6.3%. The second mass loss above 680 °C, corresponding to the endothermic peak at about 620 °C, is likely to involve the sublimation of CdS NCs, with loss of 17.9% when the temperature goes up to 850 °C. The results are consistent with that of Lou's [33].

### 3.3. TEM analyses

The XRD patterns of the as-prepared samples indicate the NCs display zinc blend characteristic features, which appeared at about 26.4°, 44.1°, and 52.1° corresponding to the (1 1 1), (2 2 0), and (3 1 1) planes of the cubic phase of CdS, respectively, which is in good agreement with the standard card (JCPDF Card No. 01-075-0581).

Representative TEM images of the CdS NCs (Fig. 3) show that the particles are spherical in shape and reasonably uniform in size. The existence of clear lattice planes in the picture (HRTEM, inset) confirms that the nanoparticles have good crystallinity. Their lattice spacing are 0.337 nm, 0.329 nm, 0.342 nm and 0.287 nm, corre-

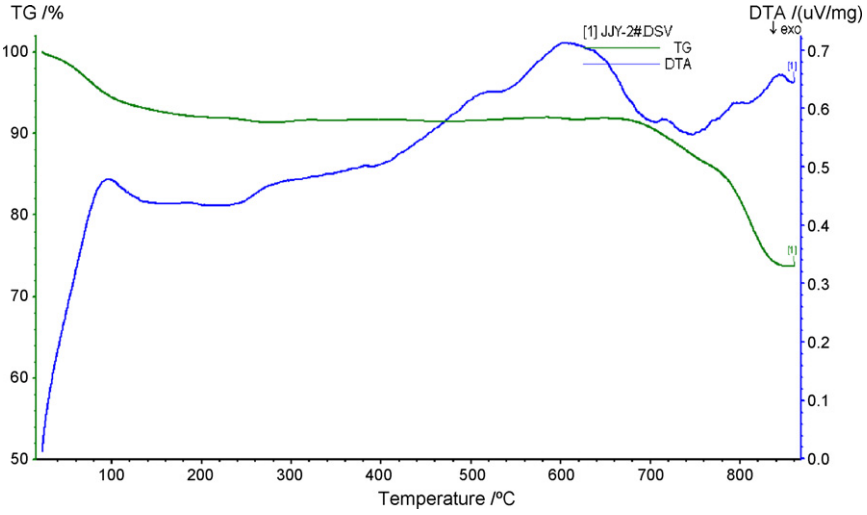


**Fig. 2.** TG–DTA curve of CdS NCs synthesized in ultrapure water at 31 °C under purity nitrogen.

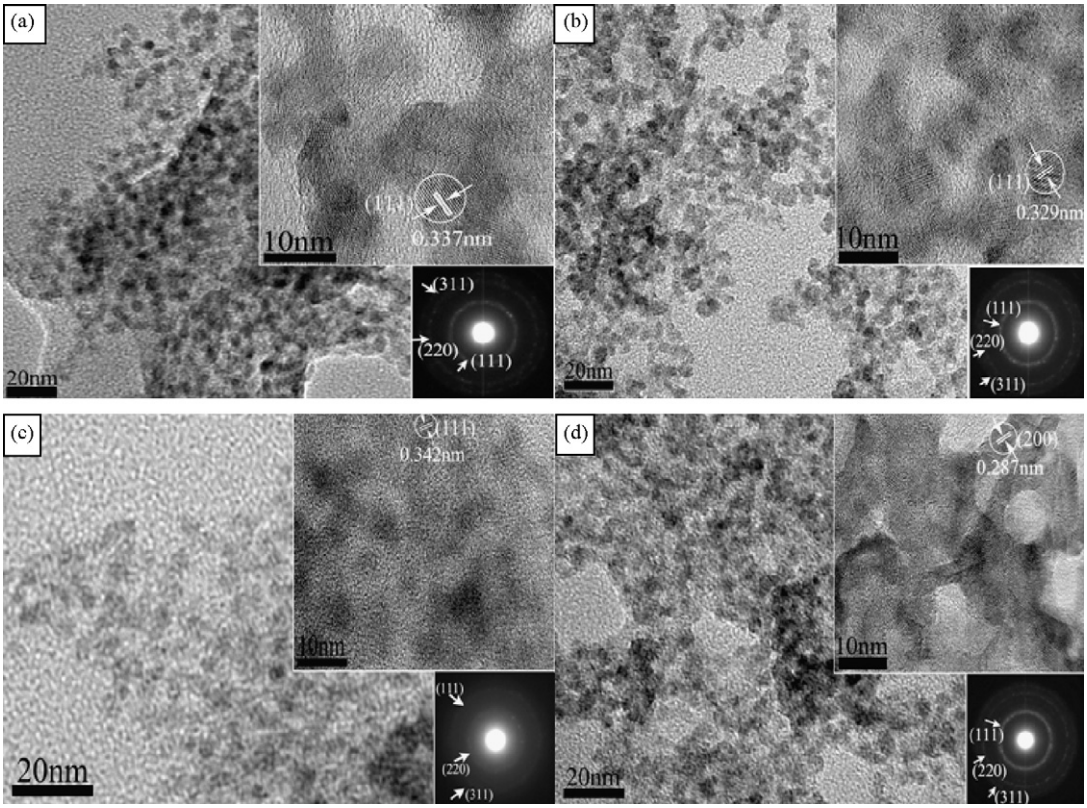


**Fig. 3.** (a and b) TEM images, HRTEM images (inset) and electron diffraction patterns (inset) of CdS NCs in ultrapure water and in ethylene glycol at 25 °C, respectively. (c and d) TEM images, HRTEM images (inset) and electron diffraction patterns (inset) of CdS NCs in ultrapure water and in ethylene glycol at 31 °C, respectively.

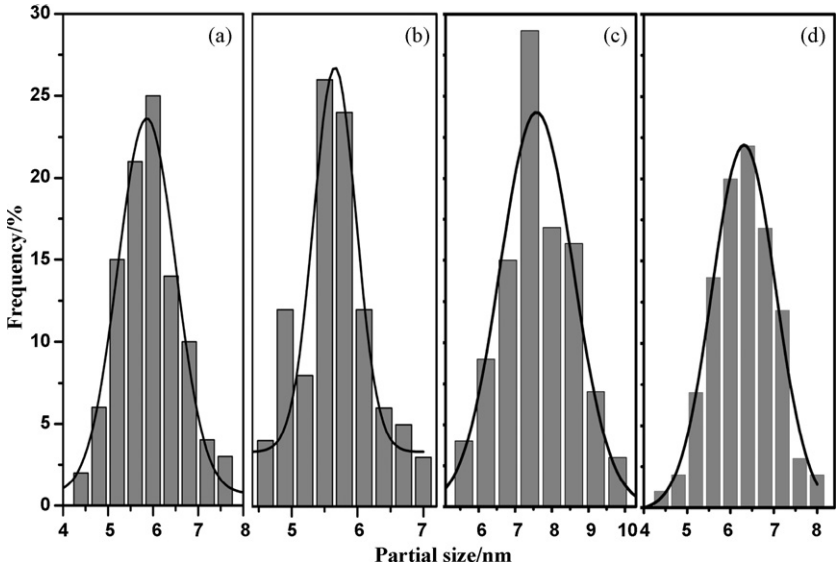


**Fig. 4.** Size distributions of CdS particles corresponding to the TEM images in Fig. 3a–d.

sponding to the (1 1 1), (1 1 1), (1 1 1) and (2 0 0) faces of cubic CdS, respectively. The SAED pattern of these nanoparticles reveals that the particles are polycrystalline in nature and the rings could be indexed based on the hawleyite cubic structure of CdS (Fig. 3, inset). From the TEM images, the particle size distributions were measured (shown in Fig. 4). The Gaussian fitting curves indicate that the main distributions of crystallite edge length are about 5.8 nm (Fig. 4a), 5.6 nm (Fig. 4b), 7.4 nm (Fig. 4c) and 6.3 nm (Fig. 4d), so it can be concluded that when the conditions are different, the mean size of the particles changes accordingly.

## 4. Conclusion

In summary, well-dispersed and uniform CdS NCs with mean size between 5.6 nm and 7.4 nm were successfully prepared. The growth thermodynamics of CdS NCs have been investigated by ITC in aqueous and ethylene glycol buffer solutions at 25 °C and 31 °C. TG/DTA method was also utilized to evaluate the thermal stability of CdS NCs in purity nitrogen. This work proved that ITC can be used as a sensitive research tool for examining the growth thermodynamic parameters of CdS NCs and the size of CdS nanoparticles

could be controlled by reaction temperatures and solvents. This facile approach is expected to study the thermodynamic properties of other inorganic materials to realize controlled synthesis by selecting appropriate solvents, temperatures, concentrations and so on. Further studies of the thermodynamics, growth mechanism and characterization experiments are underway.

## Acknowledgments

This work is financially supported by the National Natural Science Foundation of China (No. 20963001); Guangxi Natural Science Foundation of China (Nos. 0575030 and 0832078). The work is also financially supported by the National Basic Research Program of China (No. 2009CB939705).

## References

[1] C.B. Murray, C.R. Kagan, M.G. Bawendi, Ann. Rev. Mater. Sci. 30 (2000) 545–610.
[2] L.S. Cavalcante, J.C. Sczancoski, R.L. Tranquilin, J.A. Varela, E. Longo, M.O. Orlandi, Particuology 7 (2009) 353–362.
[3] C.H. Chia, S. Zakaria, M. Yusoff, S.C. Goh, C.Y. Haw, Sh. Ahmadi, N.M. Huang, H.N. Lim, Ceram. Int. 36 (2010) 605–609.
[4] D.F. Peng, S. Beysen, Q. Li, J.K. Jian, Y.F. Sun, J. Jiwuer, Particuology 7 (2009) 35–38.
[5] Z.A. Peng, X.G. Peng, J. Am. Chem. Soc. 123 (2001) 183–184.
[6] F. Gao, Q.Y. Lu, S.H. Xie, D.Y. Zhao, Adv. Mater. 14 (2002) 1537–1540.
[7] X.F. Duan, Y. Huang, R. Agarwal, C.M. Lieber, Nature 421 (2003) 241–245.
[8] W.T. Yao, S.H. Yu, S.J. Liu, J.P. Chen, X.M. Liu, F.Q. Li, J. Phys. Chem. B 110 (2006) 11704–11710.
[9] Y.F. Lin, J.H. Song, Y. Ding, S.Y. Lu, Z.L. Wang, Adv. Mater. 20 (2008) 3127–3130.
[10] T.Y. Zhai, X.S. Fang, Y. Bando, Q. Liao, X.J. Xu, H.B. Zeng, Y. Ma, Nano 3 (2009) 949–959.
[11] D. Kim, S. Okahara, K. Shimura, M. Nakayama, J. Phys. Chem. C 113 (2009) 7015–7018.
[12] Y.X. Li, Y.F. Hu, S.Q. Peng, G.X. Lu, S.B. Li, J. Phys. Chem. C 113 (2009) 9352–9358.
[13] D.N. Ke, S.L. Liu, K. Dai, J.P. Zhou, L.N. Zhang, T.Y. Peng, J. Phys. Chem. C 113 (2009) 16021–16026.
[14] P. Thakur, S.S. Joshi, S. Kapoor, T. Mukherjee, Langmuir 25 (2009) 6334–6340.
[15] J.S. Jang, U.A. Joshi, J.S. Lee, J. Phys. Chem. C 111 (2007) 13280–13287.
[16] D.J. Wang, D.S. Li, L. Gao, F. Fu, Z.P. Zhang, Q.T. Wei, J. Phys. Chem. C 113 (2009) 5984–5990.
[17] C. Wang, Y.H. Ao, P.F. Wang, J. Hou, J. Qian, S.H. Zhang, Mater. Lett. 64 (2010) 439–441.
[18] J. Puthussery, A.D. Lan, T.H. Kosel, M. Kuno, Nano 2 (2008) 357–367.
[19] C.J. Barrelet, Y. Wu, D.C. Bell, J. Am. Chem. Soc. 125 (2003) 11498–11499.
[20] C.C. Chen, C.Y. Chao, Z.H. Lang, Chem. Mater. 12 (2000) 1516–1518.
[21] Y. Liang, C. Zhen, D. Zou, D.J. Xu, J. Am. Chem. Soc. 126 (2004) 16338–16339.
[22] X.Y. Shi, S.B. Han, R.J. Sanedrin, C. Galvez, D.G. Ho, B. Hemandez, Nano Lett. 2 (2002) 289–293.
[23] X.J. Zhang, Q.R. Zhao, Y.P. Tian, Y. Xie, Cryst. Growth Des. 4 (2004) 355–359.
[24] S. Bjelic, L. Jelesarov, J. Mol. Recognit. 21 (2008) 289–312.
[25] A.L. Feig, Biopolymers 87 (2007) 293–301.
[26] S.W. Homans, Top. Curr. Chem. 272 (2007) 51–82.
[27] J.E. Ladbury, Acta Crystallogr. D 63 (2007) 26.
[28] K. Biswas, N. Varghese, C.N.R. Rao, J. Mater. Sci. Technol. 24 (2008) 615–627.
[29] N. Varghese, S.R.C. Vivekchand, A. Govindaraj, C.N.R. Rao, Chem. Phys. Lett. 450 (2008) 340–344.
[30] A. Meister, S. Drescher, I. Mey, M. Wahab, G. Graf, J. Phys. Chem. B 112 (2008) 4506–4511.
[31] J.E. Ladbury, B.Z. Chowdhry, Chem. Biol. 3 (1996) 791–801.
[32] E. Merabet, G. Ackers, Biochemistry 34 (1995) 8554–8563.
[33] W.J. Lou, M. Chen, J. Mater. Sci. Eng. 23 (2005) 891–984.